Technique for Reducing the Effects of Non-Linear Terms on Electric Field Measurements from Aircraft Platforms

Douglas M. Mach[1,*]

1. Universities Space Research Association, Huntsville, AL 35805, U.S.A.

ABSTRACT: A generalized technique has been developed that reduces the contributions of non-linear effects such as aircraft charging in the determination of the external electric fields measured by an array of field mills on an aircraft. The method uses the multiple independent measurements of the external electric field obtained during flight to determine and remove non-linear contaminations in the external vector electric field. It expands upon the technique used previously to determine the external electric field by applying linear combinations of the field mill outputs wherein each field mill output was treated as an independent measurement. To demonstrate the technique, a simulated case with non-linear contaminations was created and then corrected for the non-linear components. In addition, data from two different field programs utilizing two different aircraft and field mill configurations, each containing observable and different non-linear effects, were also corrected for the significant non-linear effects found in the field mill outputs. The expanded independent measurements in this new technique allow the determination and correction of components in the field mill outputs from almost any measurable source. Alternate utilization of the technique can include removing effects in the aircraft charge such as aircraft altitude, cloud properties, engine power settings, or aircraft flap deployment. This technique provides a way to make more precise measurements of the true external electric field for scientific studies of cloud electrification.

INTRODUCTION

Measurements of electric fields within clouds have been made using aircraft for many years [e.g., Winn, 1993; Merceret et al., 2008; Mach et al., 2009]. Retrieving electric field components from the raw aircraft field mill data while in cloud is perhaps the most difficult aspect of the measurement process because of the usually high charging of the aircraft [e.g., Jones, 1990; Koshak et al., 1994; Koshak, 2006; Koshak et al., 2006; Mach and Koshak, 2007]. The electric field as measured by an instrument on the aircraft includes linear components from the external electric field e_X, e_Y, e_Z, charge on the aircraft (e_Q), mill DC offset, and various other phenomenon, including measurement errors and non-linear terms (λ). While in cloud, these terms are often dominated by the aircraft charge, thus making it difficult to extract the ambient electric field. Note that these components of the electric field are in the reference frame of the aircraft. This study introduces a method that can detect, and greatly reduce the effects of the

* Contact information: Douglas M. Mach, Universities Space Research Association, NSSTC, 320 Sparkman Drive, Room 4022, Huntsville, Alabama, U.S.A., Email: dmach@nasa.gov

non-linear terms when they become large enough to mask the external electric fields.

LINEAR CALIBRATION METHOD

Typically, aircraft are equipped with multiple electric field mills [Bateman et al., 2007] to indirectly sense the atmospheric electric field. Note that the field mills do not directly measure the external electric fields, but instead measure the fields induced on the aircraft by the external fields and charge on the aircraft. The equation relating the output of the i^{th} mill (a_i) to the external electric field components can be represented by:

$$a_i = M_{ix}e_X + M_{iY}e_Y + M_{iZ}e_Z + M_{iQ}e_Q + M_{iD} + \lambda_i + \varepsilon_i \quad (1)$$

where the various $\mathbf{M}$ coefficients are the responses of the field mills to the external field and charge on the aircraft, M_{iD} is the DC offset of the i^{th} field mill, λ_i are the nonlinear components, and ε_i are the measurement errors. The λ_i term can include anything from aircraft corona effects (i.e., aircraft in high electric fields may emit corona ions from parts of the aircraft that are detected by the field mills) to engine thrust or aircraft angle of attack effects; these depend on engine and/or pilot input settings, not the external electric field.

For most techniques [e.g., Koshak et al., 1994; Koshak, 2006; Mach and Koshak, 2007], the non-linear terms are neglected so that the system can be solved with a linear algebraic approach:

$$a_i = M_{ix}e_X + M_{iY}e_Y + M_{iZ}e_Z + M_{iQ}e_Q + M_{iD} + \varepsilon_i \quad . \quad (2)$$

This can be sufficient to solve for the external electric field [e.g., Mach and Koshak, 2007], but at times, non-linear effects may create contaminations that mask the true external electric field.

The resultant set of equations from (2) for all components of the electric field and field mill outputs can be represented by a matrix equation:

$$\mathbf{a}(t) = \mathbf{M}\mathbf{e}(t) + \boldsymbol{\varepsilon} \quad , \quad (3)$$

where $\mathbf{a}(t)$ is the vector of field mill outputs as a function of time:

$$\mathbf{a}(t) = \begin{bmatrix} a_1(t) \\ a_2(t) \\ a_3(3) \\ \vdots \\ a_m(t) \end{bmatrix} \quad , \quad (4)$$

$\mathbf{e}(t)$ is the vector external electric field (including the charge on the aircraft) as a function of time:

$$\mathbf{e}(t) = \begin{bmatrix} e_X(t) \\ e_Y(t) \\ e_Z(t) \\ e_Q(t) \\ 1 \end{bmatrix} \quad , \quad (5)$$

where the "1" is used to eliminate the effects of DC offsets in the field mill outputs [Mach and Koshak, 2007], $\mathbf{M}$ is the m x 5 calibration matrix:

$$\mathbf{M} = \begin{bmatrix} M_{1X} & M_{1Y} & M_{1Z} & M_{1Q} & M_{1D} \\ M_{2X} & M_{2Y} & M_{2Z} & M_{2Q} & M_{2D} \\ & & \cdots & & \\ M_{mX} & M_{mY} & M_{mZ} & M_{mQ} & M_{mD} \end{bmatrix} , \quad (6)$$

and again $\boldsymbol{\varepsilon}$ are the vector measurement errors. As given in (3), the matrix $\mathbf{M}$ relates the field mill outputs to the external electric field and charge on the aircraft. Detailed descriptions of all of the components of (5) and (6) are in Mach and Koshak [2007]. The matrix $\mathbf{M}$ is constant and unique for each aircraft and field mill distribution [Mach and Koshak, 2007]. Given $\mathbf{M}$ and assuming measurement errors (ε) are small, one can directly determine the outputs of the field mills on the aircraft based on the external electric field vector. Inverting this matrix, by applying the Moore Penrose (MP) 'pseudoinverse' [Penrose, 1955], produces the $\mathbf{C}$ matrix. The elements of $\mathbf{C}$ are similar to the elements of $\mathbf{C}$ in that they relate the field mill outputs (including DC offsets) to the external electric field and aircraft charge. For example, e_X is related to the field mill outputs by:

$$e_X(t) = C_{X1}a_1(t) + C_{X2}a_2(t) + C_{X3}a_3(t) + \cdots + C_{Xm}a_m(t) \ , \quad (7)$$

where the various C's are the first row of the $\mathbf{C}$ matrix. The full version of (7), including all components is:

$$\mathbf{e}(t) = \mathbf{C}\mathbf{a}(t) \ , \quad (8)$$

where $\mathbf{a}(t)$ and $\mathbf{e}(t)$ are defined in (4) and (5). The $\mathbf{C}$ matrix is defined analogous to the $\mathbf{M}$ matrix as:

$$\mathbf{C} = \begin{bmatrix} C_{X1} & C_{X2} & C_{X3} & C_{X4} \cdots C_{Xm} \\ C_{Y1} & C_{Y2} & C_{Y3} & C_{Y4} \cdots C_{Ym} \\ C_{Z1} & C_{Z2} & C_{Z3} & C_{Z4} \cdots C_{Zm} \\ C_{Q1} & C_{Q2} & C_{Q3} & C_{Q4} \cdots C_{Qm} \\ C_{D1} & C_{D2} & C_{D3} & C_{D4} \cdots C_{Dm} \end{bmatrix} . \quad (9)$$

The electric field solution in (8) is termed the least-squares solution because it minimizes the residual $|\mathbf{a}(t) - \mathbf{M}\mathbf{e}(t)|$ [Mach and Koshak, 2007]. The $\mathbf{C}$ matrix allows the external electric field to be determined based on the field mill outputs given a properly determined $\mathbf{M}$ matrix.

Given the assumption that the field mill outputs are only a linear combination of the external electric fields, aircraft charge, and measurement errors, the intermediate estimates of the external electric field components and aircraft charge can be considered a summation of the true field component plus contaminations from other components. For example, the equation for the X component of the estimated field is:

$$f_X(t) = H_{XX}e_X(t) + H_{XY}e_Y(t) + H_{XZ}e_Z(t) + H_{XQ}e_Q(t) + H_{XD} + \varepsilon_X' \ , \quad (10)$$

where e_X, e_Y, e_Z, and e_Q are the true field components (and aircraft charge equivalent), H_{XX} is a factor that should approach 1.0 during the iterations, the other terms H_{XY}, H_{XZ}, H_{XQ}, and H_{XD} are

the contamination factors that should approach 0.0 during the iterations (such that f_X approaches e_X plus measurement errors). The purpose of the iterations in the method of Mach and Koshak, [2007] is to reduce the contamination terms (H_{XY}, H_{XZ}, H_{XQ}, and H_{XD}) to zero while setting the H_{XX} term to one so that:

$$f_X(t) = e_X(t) + \varepsilon_X' \quad . \quad (11)$$

Note that in (10) and (11) if the random and systematic errors in **a** are small (ε_X'), they can be neglected. In practice, the terms for the contamination by e_Y, e_Z, and H_{XD} are easiest to remove using the results of the roll and pitch maneuvers [Mach and Koshak, 2007]. The contamination from e_Q is more difficult to remove because the field produced by a given aircraft charge is difficult to predict. Consequently, the equation usually reduces to:

$$f_X(t) = H_{XX} e_X(t) + H_{XQ} e_Q(t) \quad , \quad (12)$$

where H_{XQ} is small and H_{XX} is close to 1.0. Much of the work in refining the f_X term in Mach and Koshak [2007] is determining and removing the e_Q component. This work is further compounded when there are significant non-linear components in the system.

NON-LINEAR EFFECT REMOVAL TECHNIQUE

Figure 1 shows an intermediate step (blue plots) in the calibration method described in Mach and Koshak [2007] for the field mills mounted on a Japanese MU-300 [Whitaker, 1981; Saito et al, 2013a; Saito et al., 2013b]. The data are from the Rocket Launch Atmospheric Electricity Investigation by JAXA in Cooperation with Academia (RAIJIN) program based at Tanegashima, Japan [Saito et al, 2013a; Saito et al., 2013b]. The aircraft was flown in and around cloud features of interest to the RAIJIN project, such as developing cumulus, layered clouds, mature thunderstorms, anvils, and decaying clouds (debris clouds) in the Tanegashima, Japan area during the winters of 2012, 2013, and 2014. The recorded electric field data were then calibrated using the method of Mach and Koshak [2007].

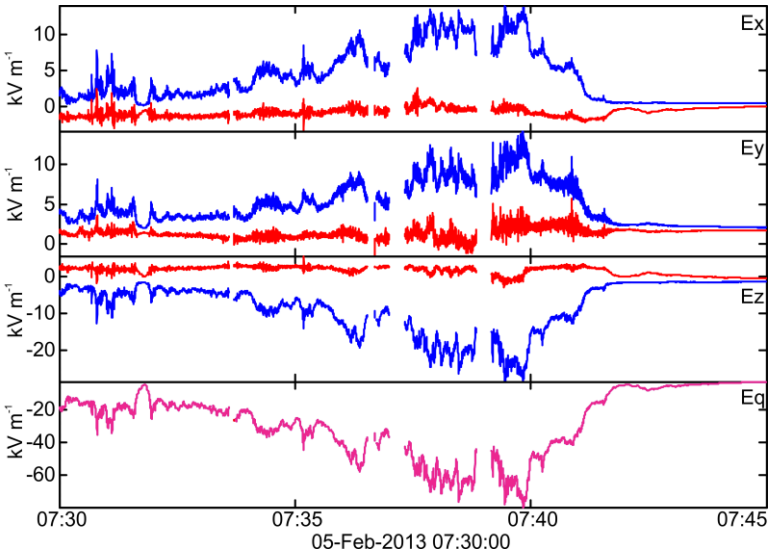

Figure 1. Electric field data components showing contamination of the $f_X(t)$, $f_Y(t)$, and $f_Z(t)$ fields by $e_Q(t)$. Note how similar the blue waveforms are compared to the $e_Q(t)$ fields. The similarities indicate that the other components ($f_X(t)$, $f_Y(t)$, and $f_Z(t)$) are contaminated by $e_Q(t)$. The red plots are the same data as the blue plots, except the $e_Q(t)$ contaminations have been removed via the linear method of Mach and Koshak [2007]. The $e_Q(t)$ term (magenta) is the same between the two datasets.

By this point in the iteration process, the cross term components (for f_X, that would be H_{XY}, H_{XZ}) have been reduced to a negligible value, with the exception of the cross term components resulting from aircraft charge (for f_X, that would be H_{XQ}, or the magenta plot in Figure 1). It is now a simple matter at this point to determine the remaining aircraft charge cross terms (H_{XQ}, H_{YQ}, and H_{ZQ}), remove them from the calibration matrix ($\mathbf{M}$), and complete the iteration process (red plots in Figure 1).

At a different time and relative e_Q magnitude (Figure 2, blue plots), however, the correction to remove the aircraft charge cross terms described in the previous paragraph has actually increased the contamination of the fields by aircraft charge (magenta plot) in the components (f_X, f_Y, and f_Z, red plots). Note that the data at this time (0600 UTC 11 February 2013) have the same calibration factor that eliminated the aircraft charge cross terms at time (0730 UTC 05 February 2013) in Figure 1 (red plots). It is the same aircraft with the same configuration of mills. If the aircraft charge cross terms varied linearly with aircraft charge and the external electric field, the $\mathbf{M}$ matrix that works at (0730 UTC 05 February 2013) should work at (0600 UTC 11 February 2013). If one plots f_X, f_Y, and f_Z as functions of e_Q (Figure 3), the problem is apparent. The plots in Figure 3 should show no pattern as f_X, f_Y, and f_Z should not have dependency on f_Q. At most, there should be a linear dependence if some of the cross terms (H_{XQ}, H_{YQ}, and H_{ZQ}) have not yet been eliminate. From (12), it is clear that in a linear system, any relationship between the estimated field components and f_Q are the results of residual H_{iQ} components. Such a relationship should be linear in f_Q. Clearly, the assumption that the non-linear components (λ) are negligible is false. There are measureable non-linear effects (λ) present in the data.

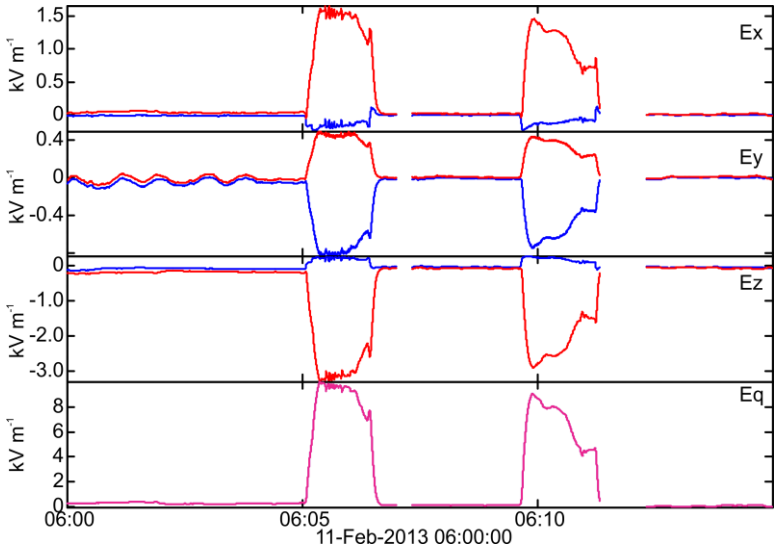

Figure 2. Electric field data from the same aircraft/field mill combination as in Figure 1, but at a different time. The blue plots use the same calibrations as the blue plots in Figure 1, with the cross contaminations of $f_X(t)$, $f_Y(t)$, and $f_Z(t)$ fields by $e_Q(t)$. The red plots have the same linear correction as the red plots in Figure 1. Notice that the correction that removed the cross contaminations in the blue plots in Figure 1 did NOT remove the contaminations for this period of time. For $f_X(t)$ and $f_Z(t)$, the linear correction (red plots) made the contaminations worse. The inability of the Mach and Koshak [2007] method to correct both time periods, with different amplitudes of $e_Q(t)$ contamination indicates the presence of non-linear contaminations.

Figure 3 actually illustrates the core concept of the technique that can be used to remove the non-linear effects from the $\mathbf{f}(t)$ function. The scatter plots in Figure 3 should show no pattern. Each of the components (f_X, f_Y, f_Z and f_Q) are similar to Eigen functions of the external electric field; they should be independent. If all cross terms H_{iQ} components are reduced to 0.0, the scatter plots in Figure 3 should ideally look more like Figure 4. The technique uses the patterns found in Figure 3 to determine the

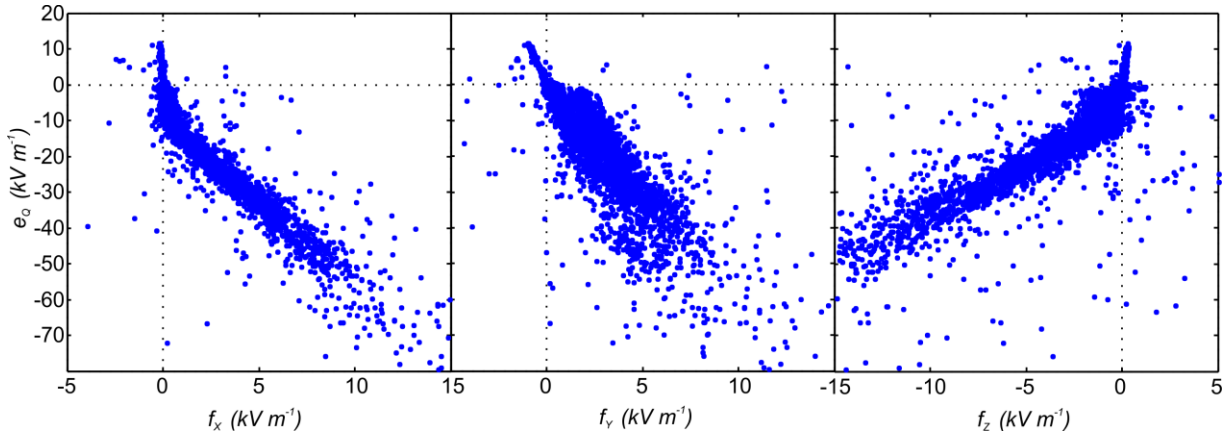

Figure 3. Plots of the components of $\mathbf{f}(t)$ as a function of $e_Q(t)$. There should be no patterns in the plots because the various components ($f_X(t)$, $f_Y(t)$, and $f_Z(t)$) should be similar to Eigen vectors of the field [Mach and Koshak, 2007]. Furthermore, if there were only linear contaminations in the data, each scatter plot would cluster around a line with zero intercept. That is not the case, indicating the presence of non-linear contaminations.

non-linear relationship between the two components. The technique then removes that non-linear relationship to create a plot more like Figure 4. The next section details the steps to remove the non-linear components.

APPLICATION AND RESULTS

First Real-World Example (MU-300)

The general pattern of λ_i seen in Figure 3 for this aircraft (Figure 5) is for a linear relationship between the field component and e_Q in the range of about +/- 10 kV/m. Outside of +/- 10 kV/m, there is a different relationship with a non-zero intercept for each external field component. Most of the dependence of $\mathbf{f}(t)$ on λ_i can be removed by fitting the data to a set of piecewise linear curves (an example of which is shown in red in

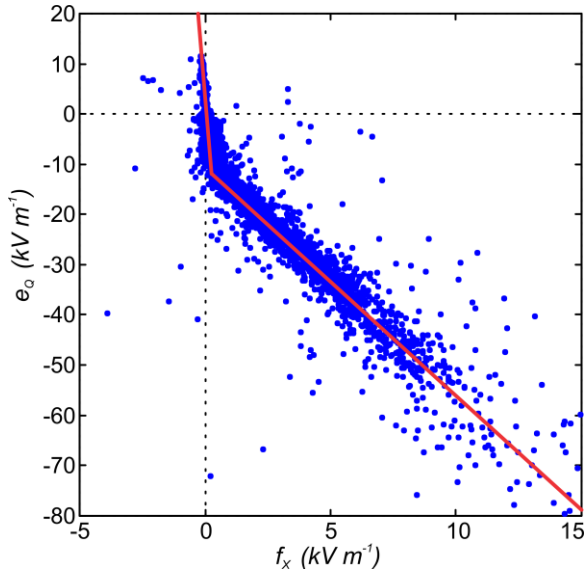

Figure 5. An example of a piecewise linear curve to remove the non-linear cross contamination of aircraft charge ($e_Q(t)$) in $f_X(t)$.

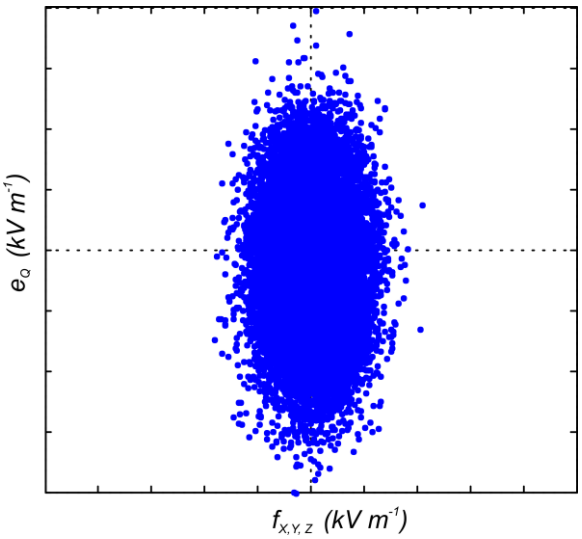

Figure 4. Ideal example (arbitrary values) where there are no cross-contaminations between the charge on the aircraft ($e_Q(t)$) and the estimations of the external electric field ($\mathbf{f}(t)$) component.

Figure 5).

The equations relating the field components and e_Q that produced the λ_i piecewise-linear curves are subtracted from the components in $\mathbf{f}(t)$ to produce scatterplots that have very little dependency on e_Q (Figure 6). For example, the equations for this specific f_X example are:

$$f'_X = f_X + 0.176 * e_Q \text{ , } e_Q > -11.71 \text{ kV m}^{-1} \quad (13)$$

and

$$f'_X = f_X + 0.2196 * (e_Q + 10.77 \text{ kV m}^{-1}) \text{ , } e_Q < -11.71 \text{ kV m}^{-1} \text{ .} \quad (14)$$

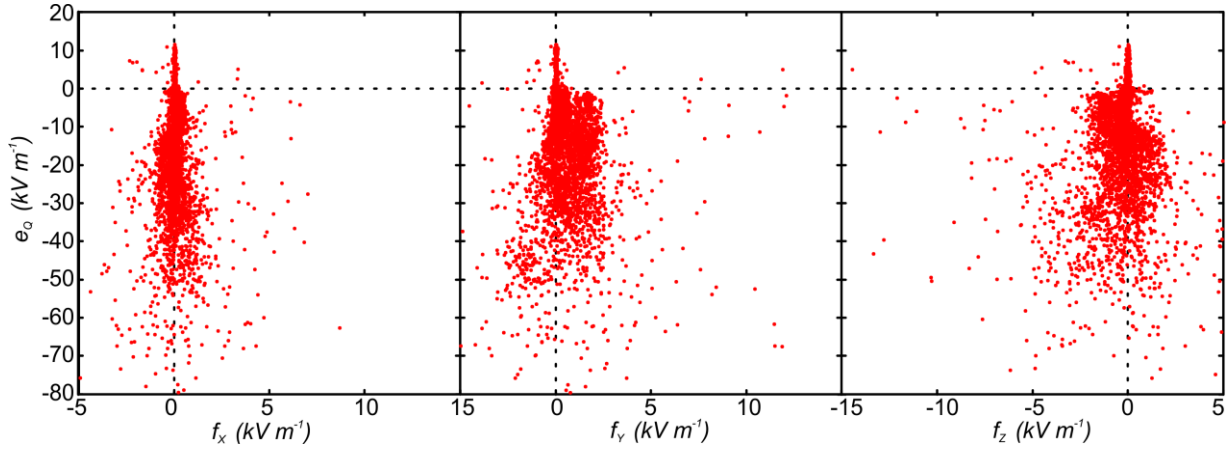

Figure 6. Same data as from Figure 3, only with the non-linear cross contaminations of $e_Q(t)$ removed. Note that there still may be contaminations in $f_Y(t)$ and $f_Z(t)$ from other unknown sources.

Figure 7 shows the same data from Figure 1, but with the non-linear components (λ_i) from (13) and (14) removed (green plots). Notice that the large e_Q terms that were present in all three components have been eliminated. Figure 8 shows the same data as in Figure 2, only with the non-linear λ_i correction from (13) and (14) removed (green plots). This section of data had a larger, erroneous e_Q component after the linear correction was used to eliminate the e_Q components from the data in Figure 1 and 3. The non-linear technique was able to remove the e_Q components from both datasets simultaneously.

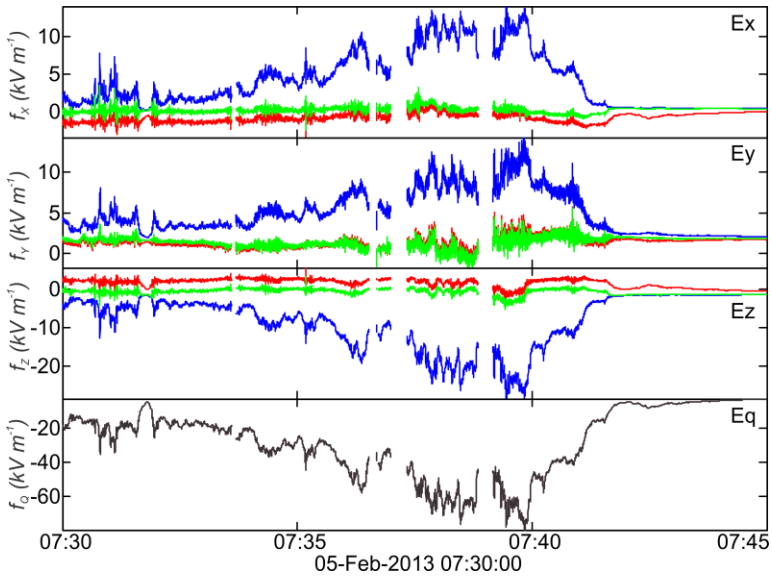

Figure 7. Comparison of the uncorrected data (blue plot), the linear method corrected data (red plot), and the non-linear method corrected data (green plot). Notice that for this data, both the linear and the non-linear techniques produce similar results.

Forward Problem Simulated Example

To more clearly illustrate how this technique works, a simulated dataset was constructed that consists of an overpass of several model charge structures. The simulated fields, **e**(t) in Figure 9 characterize an aircraft flying to one side, then through, and then to the other side of an arbitrary vertical charge distribution. The fields at the mills from aircraft charge, e_Q, are arbitrarily varied from 10.0 kV m^{-1} to -80 kV m^{-1} as is typically found in the MU-300 dataset. Figure 10 shows the same data as in Figure 9, except with a small amount of random noise added to each component to simulate measurement errors. Figure 11 shows the data from Figure 10 with added non-linear contaminations that depend on e_Q. The data in Figure 11 are now the **f**(t) data that will be analyzed using the method in this report. A major assumption at this point is that the method of Mach and Koshak [2007] has been used to eliminate all cross terms in Equation 8 except those produced by the charge on the aircraft (H_{iQ}).

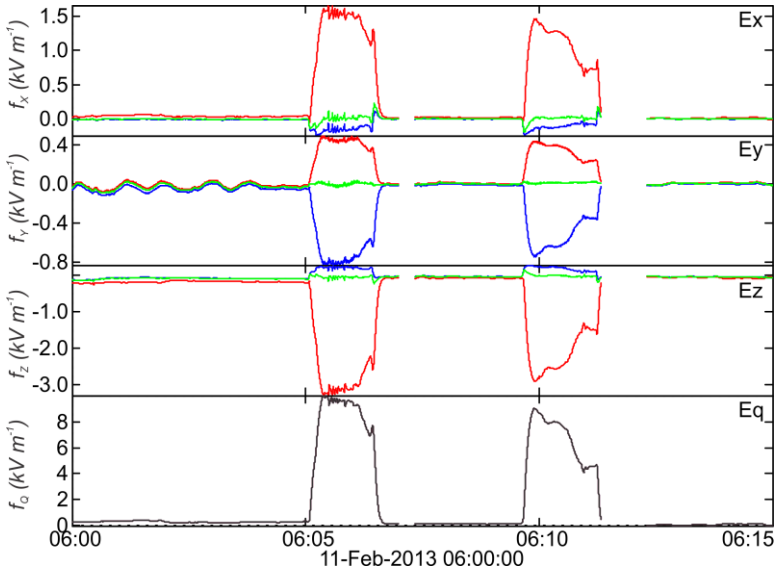

Figure 8. Comparison of the uncorrected data (blue plot), the linear method corrected data (red plot), and the non-linear method corrected data (green plot). For this time period, only the non-linear technique was able to remove the $e_Q(t)$ contamination.

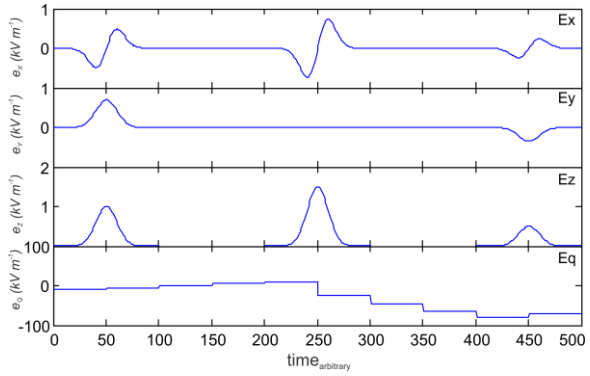

Figure 9. Simulated fields and aircraft charge profile for the example analysis. The time and field amplitudes are arbitrary.

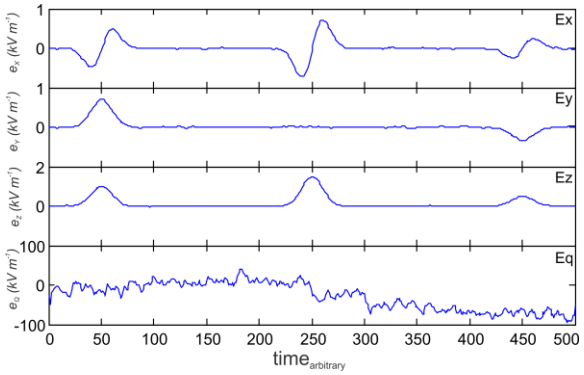

Figure 10. Simulated fields plus typical noise values to create a more realistic example.

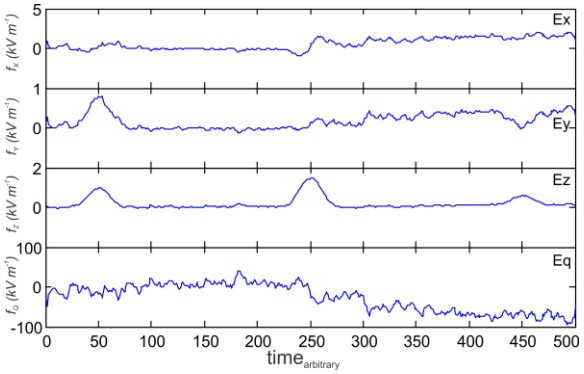

Figure 11. Estimated fields with non-linear $e_Q(t)$ components. This is the starting point of the ideal example analysis using the technique described in this study.

Figure 12 corresponds to the same plot as Figure 3. For each component, the estimated piecewise-linear fits are shown on the subfigures. These curves are subtracted from the components to

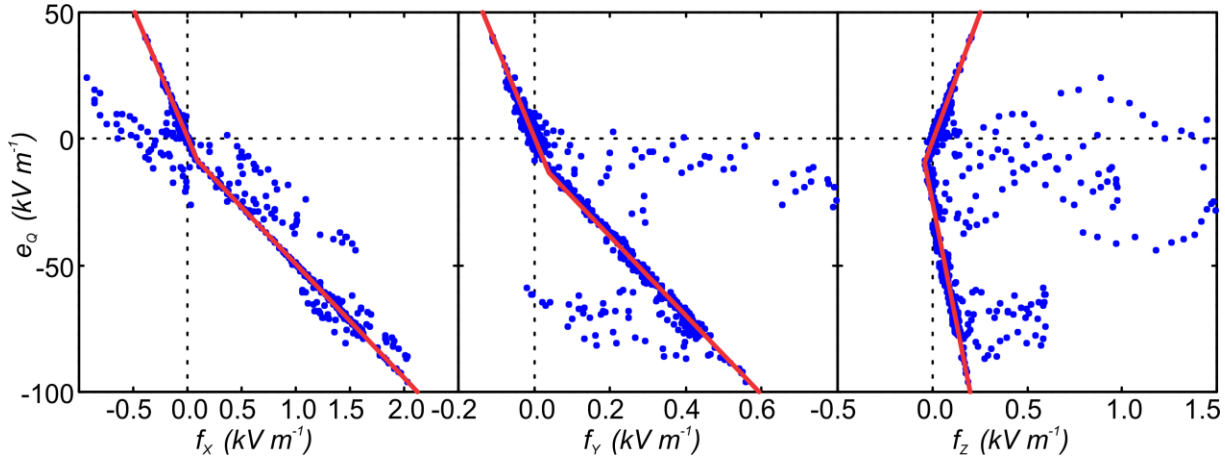

Figure 12. Plots of $\mathbf{f}(t)$ verses $e_Q(t)$ used to determine the cross contamination non-linear fits. The red curves are the fits used to remove the non-linear $e_Q(t)$ contaminations.

produce Figure 13 which has the estimated non-linear components removed. Figure 14 shows the results of the removal of the non-linear dependency, along with the original simulated dataset plus noise prior to

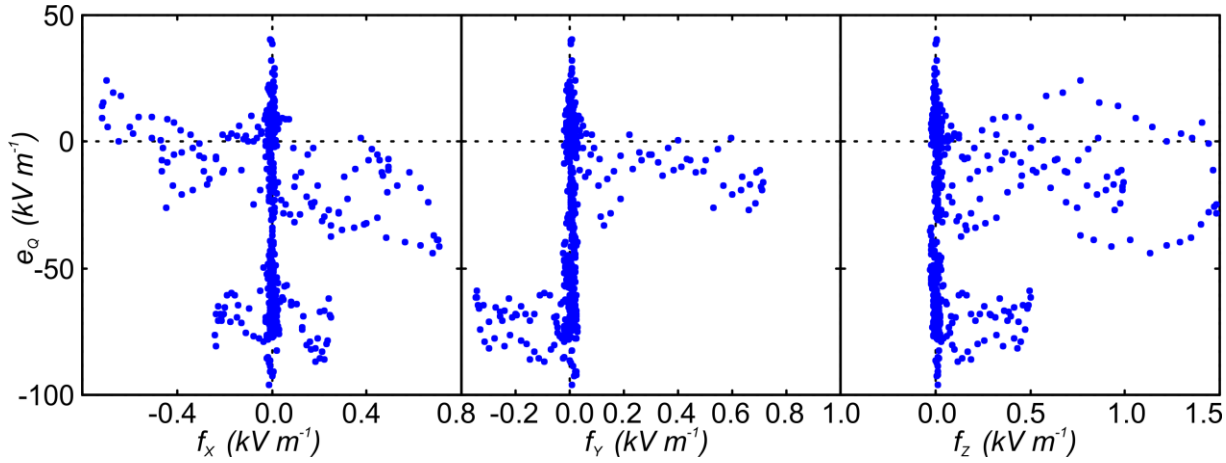

Figure 13. Plots of $\mathbf{f}(t)$ verses $e_Q(t)$ after removing the non-linear $e_Q(t)$ contaminations using the technique detailed in this report.

adding the non-linear components (data from Figure 10). Figure 15 shows the differences between the simulated fields (with noise but without the non-linear components) and the "corrected" fields. Note that the technique was able to remove the non-linear contaminations to the various simulated field components in the presence of small amounts of measurement errors (random noise). The differences in Figure 15 are on the order of the noise introduced into the data and are from errors in determining the slope and

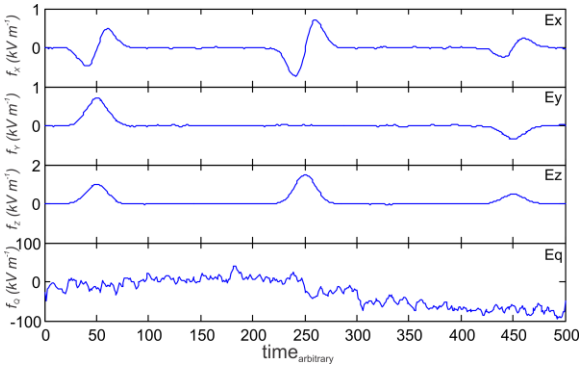

Figure 14. Corrected fields as a function of time. The non-linear $e_Q(t)$ components were removed using the technique described in this study.

intersection point for the non-linear terms.

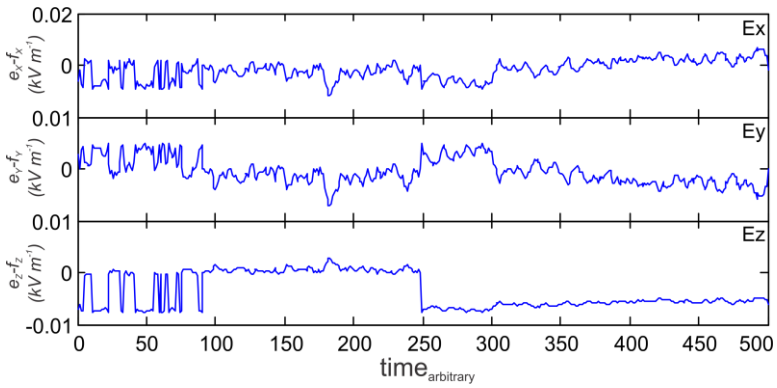

Figure 15. Difference between the ideal fields (without the $e_Q(t)$ contaminations) and the fields determined with the technique described in this study. The differences are on the order of the noise introduced into the data and are from the errors in determining the slope and intersection point for the non-linear terms.

Second Real-World Example (Citation)

A second real-world example from a different aircraft and a different field program are shown in Figures 16 and 17. The data are from the 2000-2001 Airborne Field Mill II experiment (ABFM II) that was conducted near Kennedy Space Center, Florida to measure the electric field, reflectivity, and microphysics in thunderstorm anvils (and other clouds) produced by deep convection with a Citation aircraft [Dye et al., 2007]. Figure 16 shows the uncorrected and corrected electric field vector components time series for a cloud penetration on May 22, 2001 with the North Dakota Citation [Dye et al., 2007]. Note that f_X, a term that should be more or less symmetric about zero, is unrealistically unipolar. Figure 17 shows the relationship between f_X and f_Q, indicating the presence of non-linear charging of the aircraft. The corrected data in Figure 16, f_X are now much closer to a realistic pattern with symmetry about zero. Additionally, the plots of the various $\mathbf{f}(t)$ components versus e_Q for the two aircraft are quite different (see Figures 5 and 17).

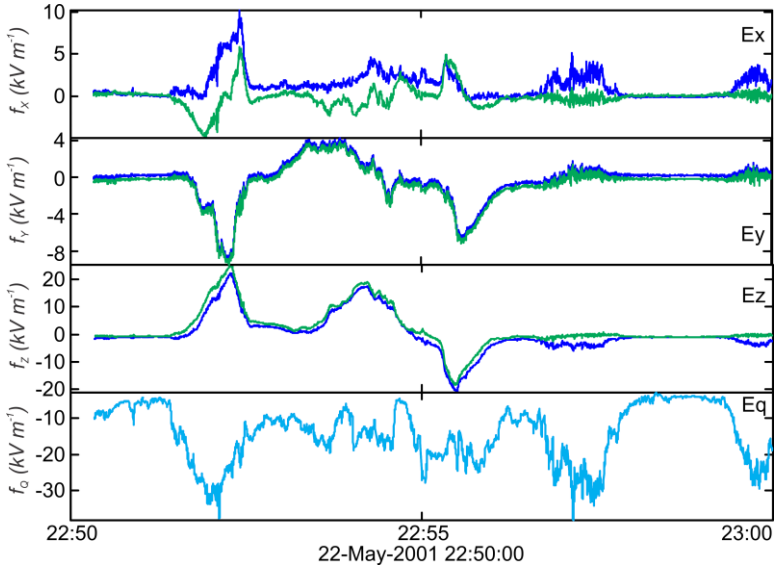

Figure 16. Plot of aircraft fields for the Citation aircraft and field mill configuration [Dye et al., 2007]. The blue curves are the uncorrected values while the green curves are corrected using the non-linear method described here. Although the non-linear effects are smaller in this case, the technique described in this study fixes the unrealistic unipolar $f_X(t)$ values.

Independent Measurements

In Mach and Koshak [2007], the linear method requires at least as many field mills as components. For example, with four components (e_X, e_Y, e_Z, and e_Q), at least four field mills are required. Determining higher order components, such as non-linear ones, was impossible because there simply were too few field mills. The method described in this work uses the same number of field mills, yet is able to

determine many more components (the various non-linear terms) of the electric field than there are mills.

This is possible because there are multiple independent measurements of the electric field during a flight. Figure 18 shows the autocorrelation functions for the ABFM Citation dataset [Dye et al., 2007] and the MU-300 [Whitaker, 1981]. The autocorrelation coefficient (r) drops below 1/e for both sets of data by about 150 s, indicating that measurements made at longer intervals than that are uncorrelated [Leith, 1973; Rudlosky and Fuelberg, 2013]. Electric field measurements made at intervals longer than ~2.5 minutes are essentially independent; subsequently, in a 90 minute flight, there are over 200 independent samples of the electric field (one sample every 2.5 minutes and 6 field mills). More independent data can be obtained across multiple flights as long as the aircraft configuration is constant. These numbers of independent measurements are sufficient to be able to detect and remove non-linear components of the electric field by this technique.

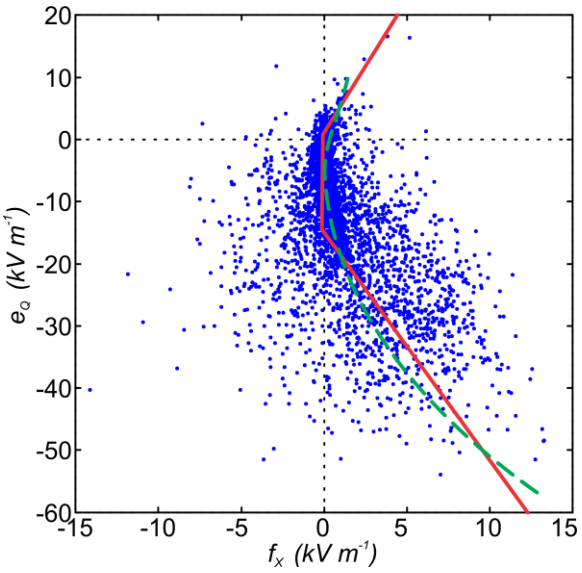

Figure 17. Uncorrected plot of $e_Q(t)$ verses $f_X(t)$ for the data from Figure 16. Although the non-linear components are smaller for this aircraft and field mill configuration, the non-linear terms are still present and can be corrected using the technique from this study. For the corrected data in Figure 16, the red piecewise-linear correction (red curve) was used. It is possible that a quadratic fit (green curve) might provide a better fit. Either non-linear correction can be detected with the technique from this study.

SUMMARY

The technique described in this report utilizes the large number of independent measures of the electric field across all field mills that are available on an aircraft. The independent measurements are used to detect and then remove contaminations in the estimates of the true external electric field in the presence of small random measurement errors. The method is applied after the best linear calibration matrix (**M**) is found using the technique of Mach and Koshak [2007]. The **M** matrix results are then used as a basis for determining and then removing the remaining linear and non-linear terms that might still be present. The technique was demonstrated on two actual aircraft field datasets and one simulated

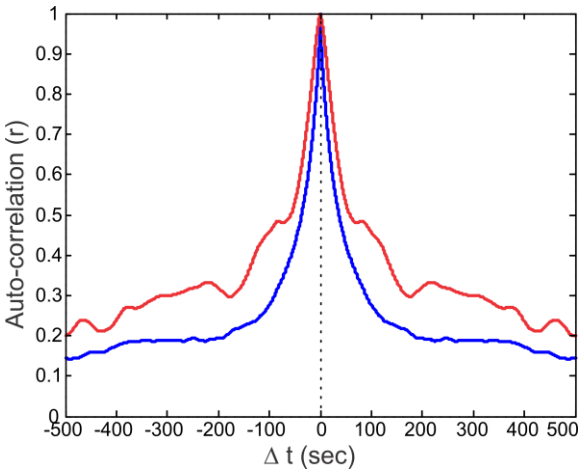

Figure 18. Auto-correlation of the aircraft electric field component ($f_X(t)$), indicating a lack of correlation for both datasets after only ~150 seconds (r < 1/e). The blue curve is from the Citation data, while the red curve is from the MU-300 data.

dataset.

This technique can be used on any aircraft/field mill combination where the linear method proves to be inadequate to remove all cross terms and non-linear effects. It should be noted that this technique can also be used to determine more complex non-linear components than were used here. An example is the parabolic function as seen in the green curve in Figure 17. Given the number of independent measurements found in a typical flight, there is ample data to fit a quadratic non-linear term to correct the contaminations in the external electric field measurements.

In this report, contaminations in the external electric fields resulting from aircraft charge were detected and removed. Other sources of contamination, such as engine power settings or flap positions that can contribute to the aircraft self-charge can be detected and removed using this technique. The only requirement is that the source of the contamination be measurable as a function of time against the external electric field components. A possible example is illustrated in Figure 6. The multiple vertical lines in the f_X plot indicate the presence of a term that depends on aircraft parameters other than e_Q. If a plot of the external source and the electric field component indicates a pattern, the effect of the contamination can be detected and removed.

ACKNOWLEDGMENTS

The author gratefully acknowledges the support received from the Japan Aerospace Exploration Agency (JAXA) Space Transportation Mission Directorate, the sponsor of this airborne field measurement campaign. In addition, the author would like to thank the individuals from the collaborating organizations that contributed to the data used in this analysis. Collaborators include the University of Alabama in Huntsville, Universities Space Research Association, NASA Marshall Space Flight Center (MSFC), Mitsubishi Heavy Industry, and Diamond Air Service. I would like to also thank Dr. William Koshak of MSFC for his help in checking the mathematical formulas employed in the study.

REFERENCES

Bateman, M. G., M. F. Stewart, R. J. Blakeslee, S. J. Podgorny, H. J. Christian, D. M. Mach, J. C. Bailey, and D. Daskar, 2007: A low-noise, microprocessor-controlled, internally digitizing rotating-vane electric field mill for airborne platforms, J. Atmos. Ocean. Tech., 24, pp. 1245–1255, doi: 10.1175/JTECH2039.1.

Dye J. E., M. G. Bateman, H. J. Christian, E. Defer, C. A. Grainger, W. D. Hall, E. P. Krider, S. A. Lewis, D. M. Mach, F. J. Merceret, J. C. Willett, and P. T. Willis, 2007: Electric fields, cloud microphysics, and reflectivity in anvils of Florida thunderstorms, J. Geophys. Res., 112, D11215, doi:10.1029/2006JD007550.

Jones, J. J., 1990: Electric charge acquired by airplanes penetrating thunderstorms, J. Geophys. Res., 95, 16589-16600.

Koshak, W. J., J. C. Bailey, H. J. Christian, and D. M. Mach, 1994: Aircraft electric field measurements: Calibration and ambient field retrieval, J. Geophys. Res., 99, 22781-22792.

Koshak, W. J., 2006: Retrieving storm electric fields from aircraft field mill data. Part I: theory, J. Atmos. Oceanic Technol., 23, 1289-1302.

Koshak, W. J., D. M. Mach, H. J. Christian, M. F. Stewart, M. Bateman, 2006: Retrieving storm electric fields from aircraft field mill data. Part II: applications, J. Atmos. Oceanic Technol., 23, 1303-1322.

Leith, C. E., 1973: The standard error of time-average estimates of climate means, J.Appl. Meteor.,12, 1066-1069.

Mach, D. M. and W. J. Koshak, 2007: General matrix inversion technique for the calibration of electric field sensor arrays on aircraft platforms, J. Atmos. Ocean. Tech., 24, pp. 1576–1587, doi:10.1175/JTECH2080.1.

Mach, D. M., R. J. Blakeslee, M. G. Bateman, and J. C. Bailey, 2009: Electric fields, conductivity, and estimated currents from aircraft overflights of electrified clouds, J. Geophys. Res., 114, D10204, doi:10.1029/2008JD011495.

Merceret, F. J., J. G. Ward, D. M. Mach, M. G. Bateman, and J. E. Dye, 2008: On the magnitude of the electric field near thunderstorm-associated clouds, J. Appl. Meteor. Clim., 47, 240– 248.

Penrose, R., 1955: A generalized inverse for matrices, Proc. Cambridge Philos. Soc. 51, 406-413.

Rudlosky, S. D., and H. E. Fuelberg, 2013: Documenting storm severity in the Mid-Atlantic region using lightning and radar information, Mo. Wea. Rev., 141, 3186-3202,DOI: 10.1175/MWR-D-12-00287.1.

Saito, T., Y. Saito, and K. Okita, 2013a: Results of RAIJIN2012, the intensive observation program to relax the triggered lightning launch commit criteria, 16th Conference on Aviation, Range, and Aerospace Meteorology, Austin, TX, Amer. Meteor. Soc., J3.5.

Saito, Y., T. Saito, and K. Okita, 2013b: Proposal of new triggered lightning launch commit criteria for Japan’s safety rocket launch, 6th IAASS Conference, Montreal, Canada, International Association for the Advancement of Space Safety, 12.3.1.

Whitaker, Richard, 1981: Diamond 1: Mitsubishi's first business jet, Flight International, 18 July, pp. 163–170.

Winn, W. P., 1993: Aircraft measurement of electric field: Self calibration. J. Geophys. Res., 98, 7351–7365.